Hydrological sensitivity of the Adour-Garonne river basin to climate change

Yvan Caballero, Sophie Voirin-Morel, Florence Habets, Joël Noilhan, Patrick Lemoigne, Alain Lehenaff, Aaron Boone

Hydrological sensitivity of the Adour-Garonne river basin to climate change

Yvan Caballero,[1] Sophie Voirin-Morel,[2] Florence Habets,[3] Joël Noilhan,[4] Patrick LeMoigne,[4] Alain Lehenaff,[4] and Aaron Boone[4]

Received 16 April 2005; revised 7 March 2007; accepted 28 March 2007; published 28 July 2007.

[1] Output atmospheric fields from seven global climate models (GCMs) were extracted over a domain covering the Adour-Garonne basin in southwestern France in order to calculate precipitation and temperature anomalies for the decade 2050–2060 relative to the present climate. These anomalies showed a general trend of increasing precipitation in wintertime and decreasing precipitation in summertime, together with an increase in the annual average temperature of approximately 2°C. The anomalies were used to create seven modified climate-forcing data sets, which were then used to drive the SAFRAN-ISBA-MODCOU (SIM) hydrometeorological modeling system. The river discharge simulated by the SIM model under each modified climate for the 2050–2060 decade was compared to the discharge simulated for the 1985–1995 reference decade. The results show a slight decrease in the low river flow, on the order of 11% ± 8% on average for all of the climate-forcing data sets and the hydrometric stations. However, there was a significant impact on the snowpack in terms of reduced snow cover depth and duration. These changes provoked a discharge decrease in the spring and a large increase in winter due to the additional liquid precipitation. Considering the large range in climate conditions of the period studied, it appears that the hydrological sensitivity of the river basin is greater when applying the same climate modification to a wet year as opposed to a dry year. Finally, a transient climate forcing covering the 1985–2095 period provokes a general tendency to decrease the river discharge for all seasons.

Citation: Caballero, Y., S. Voirin-Morel, F. Habets, J. Noilhan, P. LeMoigne, A. Lehenaff, and A. Boone (2007), Hydrological sensitivity of the Adour-Garonne river basin to climate change, *Water Resour. Res.*, *43*, W07448, doi:10.1029/2005WR004192.

1. Introduction

[2] The reality of climatic change related to the increase in the principal greenhouse gas concentrations (carbon dioxide, CO_2, methane, CH_4, nitrous oxide, N_2O) and chlorofluorocarbons (CFCs) over the industrial period is now generally accepted by the scientific community. Some of the evidence of the climatic response to this increase, summarized in the Intergovernmental Panel on Climate Change (IPCC) report [*Houghton et al.*, 2001], are a global atmospheric temperature increase (0.6 ± 0.2°C since the end of the 19th century, twice as high over the continents as over the oceans); a global precipitation increase over the Northern Hemisphere's middle and high latitudes and a decrease over the tropical zones; an increase in the water vapour content of the low troposphere and in the extreme precipitation event frequency over the USA and England [*Palmer and Räisänen*, 2002; *Caballero and Noilhan*, 2003]; a global snow cover decrease on the order of 10% since 1960 and a reduction in river and lake freezing period duration of approximately 2 weeks; and a 1- to 2-mm/year sea level rise during the 20th century.

[3] A number of studies have analyzed observed hydrologic trends and their connections with the changing climate. A study from the California Department of Water Resources [*Stewart et al.*, 2005] concludes that the fraction of total annual runoff occurring in the late-April-to-July period has been decreasing over the past century in the Sacramento/San Joaquin river basins, with no apparent trend in total runoff. Some studies, which focused on the river discharge from more than 200 gauges with a minimum record length of 25 years, found different results depending on the geographic situation, implying that the impacts are not spatially uniform. For instance, the annual runoff decrease in the southern part of Canada is different from the increase in the northern part of the country. Moreover, a monthly runoff increase in the March-to-April period and a decrease during summer were observed in the same country [*Burn and Hag Elnur*, 2002]. In Europe, some studies have observed trends that have been found to be different from low-frequency natural variability. With temperature, for example, the increase seems to have been more intense in summer than in winter over the last century, and it varies

[1] French Geological Survey (BRGM), Immeuble Agostini, Z.I. de Furiani, Bastia, France.
[2] Direction of Climatology, Météo-France, Toulouse, France.
[3] UMR Sisyphe École des Mines de Paris (ENSMP), Fontainebleau, France.
[4] Centre National Recherche Meteorologique, Météo-France, Toulouse, France.

0043-1397/07/2005WR004192

according to the geographic location. In France, it is more pronounced in the south (for certain years it is more than 1°C) than in the north (0.6–0.7°C) [*Moisselin et al.*, 2002]. In southern Europe, the precipitation rate decrease was estimated to be 20% during the 20th century. For example, a successive drying of the most sensitive areas of Catalonia and Andalučacute;a to the winter Atlantic depressions has been observed on a precipitation data set of the 30-year period (1964–1993) divided into three decades [*Romero et al.*, 1998]. A considerable increase in winter rainfall has been observed in the Alzette River basin in Luxembourg over the past 50 years [*Drogue et al.*, 2004]. In France, even though both a precipitation increase in winter and a decrease in summer have been observed, no particular trend was found for the annual budget [*Moisselin et al.*, 2002]. Most of the predicted responses to the greenhouse gas increases, largely based on General Circulation Model (GCM) simulations, indicate that the observed trends will persist and even be amplified in the future. These responses include increases in surface air temperature (IPCC's conclusions predict a surface temperature increase from 1.5 to 5°C by 2100) and global mean rates of evaporation, rising sea level, and changes in the biosphere. Although most of the simulations predict a general and global increase in precipitation for higher latitudes during rainy seasons and a decrease for the lower latitudes during dry seasons, the results can be very different depending on the season and geographic situation considered. *Gregory et al.* [1997] found, for example, no change in the precipitation rate in winter and 20% less precipitation in the summer over southern Europe with a simulation using twice the current level of atmospheric CO_2 (the other greenhouse gases remaining constant). Other studies simulate precipitation decreases in Australia, Central America and South Africa in winter and in Europe in summer [*Houghton et al.*, 2001].

[4] Increasingly, many studies assess the impact of the climate change on the basis of hydrological processes. They generally conclude that there will be an intensification of seasonal variations: an increase in river discharge in winter and a reduction in summer, except for the river basins containing significant groundwater reservoirs [*Arnell and Reynard*, 1996; *Bobba et al.*, 1997; *Arnell*, 1999; *Roy et al.*, 2001; *Morin and Slivitzky*, 2002, *Miller et al.*, 2003; *Drogue et al.*, 2004], although the recharging of these reservoirs may sometimes be reduced [*Rosenberg et al.*, 1999; *Allen et al.*, 2004]; intensification of extreme floods [*Roy et al.*, 2001; *Milly et al.*, 2002; *Booij*, 2005]; and an earlier beginning of the low water level period [*Douville et al.*, 1999], mainly due to a reduction in the snow cover and an earlier spring thawing [*Martin*, 2000; *Etchevers et al.*, 2002; *Zierl and Bugmann*, 2005]. *Nash and Gleick* [1991] and *McCabe and Hay* [1995] showed that the modification of the precipitation regime has a greater impact on the discharge amplitude (difference between the minimum and the maximum value of the monthly discharge), while the modification of the atmospheric temperature intensity has a greater impact on the seasonal river flow regime (temporal evolution of the river flow). While groundwater systems are likely to delay and disperse the impacts of climate change, *Chen et al.* [2004] suggest that the predicted temperature increase for the Canadian prairies may reduce net recharge and affect groundwater levels. Again, the trends summarized can be highly variable depending on both season and geographic situation, even at the regional scale [*Gellens and Schädler*, 1997; *Zhang et al.*, 2001; *Etchevers et al.*, 2002; *Zierl and Bugmann*, 2005].

[5] This article presents the results of a study which focuses on the investigation of the possible impacts of climate change on the Adour-Garonne river basin in France. The spatially distributed and physically based hydrometeorological modeling system, SAFRAN-ISBA-MODCOU (SIM), was used at a resolution of 8 km to take into account the spatial variability of the hydrometeorological processes and the land surface hydrology. The SIM modeling system, the study area and the results of the simulation for the present hydrological state (particularly during a low-flow period), are described in section 2. Precipitation and temperature anomalies were calculated between the present (1985–1995) and the future (2050–2060) using several GCM simulations, to build the so-called atmospheric forcing scenarios for the hydrometeorological system for the period 2050–2060 (section 3). The simulated future river discharges in each atmospheric scenario were compared to the simulated present-day discharges (section 4.1). In addition, a continuous climate scenario from 1985 to 2100, provided by a recent simulation of the ARPEGE/IFS coupled ocean-atmospheric model simulation [*Gibelin and Déqué*, 2003], was used to study the continuous trend of the impact of climate change (section 4.2).

2. Modeling the Daily Hydrometeorological Situation in the Adour-Garonne River Basin

2.1. Study Area Description

[6] The Adour-Garonne river basin (116,000 km^2) is located in southwestern France and drains the northern slopes of the Pyrenean chain (along the French border with Spain), stretching eastward from the Atlantic Ocean to the Mediterranean Sea. The principal rivers of the basin are the Garonne flowing from south to north along with its main tributaries: the Ariège, the Tarn and the Lot (Figure 1), which together drain up to half the area of the basin. The Adour River drains the southwestern part of the basin, and the Dordogne River drains the northern part of the area (they are two independent basins). The Pyrenean mountain chain, with peaks higher than 3000 m, and the Massif Central region border the basin to the south and to the east, respectively. The Adour, the Garonne, and the Ariège rivers have their beginnings in foothills of the Pyrenean chain. The Tarn, the Aveyron, the Lot, and the Dordogne rivers originate in the Massif Central. An important deep groundwater reservoir, the Landes aquifer, is located beneath the vast Landes of Gascogne plain in the western part of the basin (Figure 1). The major share of the water of the aquifer flows to the west, while the bulk of the remaining water flows into the Garonne River. The intensity of human activity (agricultural and industrial) is variable over the basin, and it is most intense in the Garonne and Dordogne basins (hydroelectricity and agriculture) and in the Adour River basin (agriculture). The climate over the basin is under the influence of oceanic conditions over the western part of the domain characterized by heavy rainfall events during winter and relatively warm and humid weather during summer. The southeastern part is under the influence

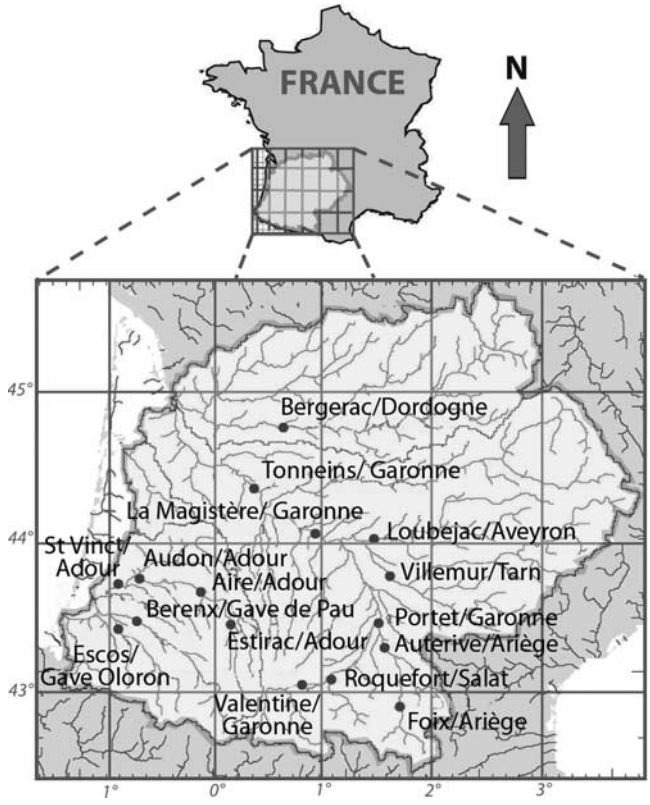

Figure 1. The Adour-Garonne river basin and location of the 16 hydrometric stations monitored.

of a Mediterranean climate, characterized by high temperatures in summer and heavy rainfall events in autumn and spring. There is a significant precipitation gradient from the west to the east, ranging from approximately 1200 mm/year in the Atlantic coastal region to about 600 mm/year 300 km to the east.

2.2. Application of the SIM System to the Adour-Garonne River Basin

2.2.1. SIM System

[7] The SAFRAN-ISBA-MODCOU (SIM) hydrometeorological modeling system was designed to simulate the surface energy and water budgets of the continental land surface, as well as the runoff routing for a given drainage network and the evolution of the main aquifers (Figure 2) for regional-scale basins. It is composed of three components, the first of which is the SAFRAN meteorological parameter analysis system [*Durand et al.*, 1993]. The second component consists in the Interactions between the soil-biosphere-atmosphere (ISBA) soil-vegetation-atmosphere-transfer (SVAT) scheme [*Noilhan and Planton*, 1989; *Noilhan and Mahfouf*, 1996; *Boone et al.*, 1999], which is also used in the global circulation, mesoscale research and operational forecast models of the French Weather Service. The final part is the macroscale distributed hydrological model MODCOU [*Ledoux et al.*, 1989]. The SAFRAN-ISBA-MODCOU (SIM) hydrometeorological modeling system has been applied to the Adour River basin [*Habets et al.*, 1999b] and to the Rhône and Seine basins [*Habets et al.*, 1999a; *Etchevers et al.*, 2001, *Rousset et al.*, 2004].

[8] SAFRAN uses all the available screen-level meteorological observations, climatic data, and operational analysis of the numerical weather prediction model of Météo-France Action Recherche Petite Echelle et Grande Echelle (ARPEGE) [*Courtier and Geleyn*, 1988]). The ARPEGE operational analysis is used as a first guess for the SAFRAN analysis in order to derive the nebulosity, and thus the incoming radiation. SAFRAN uses the optimal interpolation method [*Durand et al.*, 1993] to combine all the relevant data. The analysis then outputs the altitude-dependent profile of the screen-level parameters in each homogeneous climate zone. It was extended to all of France in 2002 [*LeMoigne*, 2002], and it was used to determine both the spatial and temporal distribution of the meteorological parameters and their evolution with altitude (which is a key for hydrological processes modeling in mountainous areas) over the Adour-Garonne river basin [*Voirin-Morel*, 2003].

[9] The ISBA scheme simulates the water and energy exchanges between the surface and the atmospheric boundary layer, the changes in the soil's water content and the runoff and deep drainage fluxes. The soil-vegetation surface energy budget is solved using physically based relations linking the thermal and hydrological properties of the soil to the texture and vegetation type. The meteorological parameters needed by ISBA are the atmospheric temperature and humidity, the short-wave and long-wave downwelling radiative fluxes, the wind speed, the solid and liquid precipitation rates and the surface atmospheric pressure. These variables are provided at 3-hourly or hourly time steps by the SAFRAN analysis system at an 8-km spatial resolution. The coefficients governing the water and energy exchanges were validated during previous studies using data from field

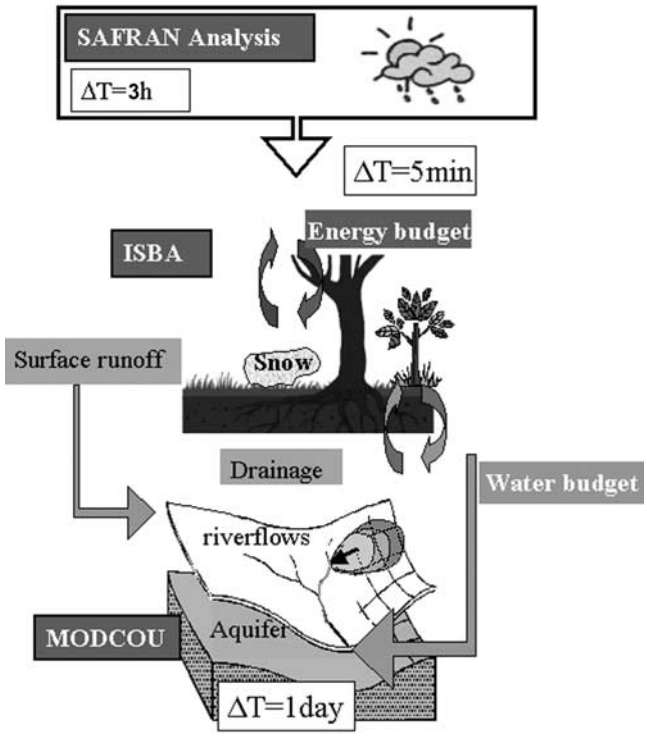

Figure 2. SAFRAN-ISBA-MODCOU (SIM) structure and links (ΔT is the time step).

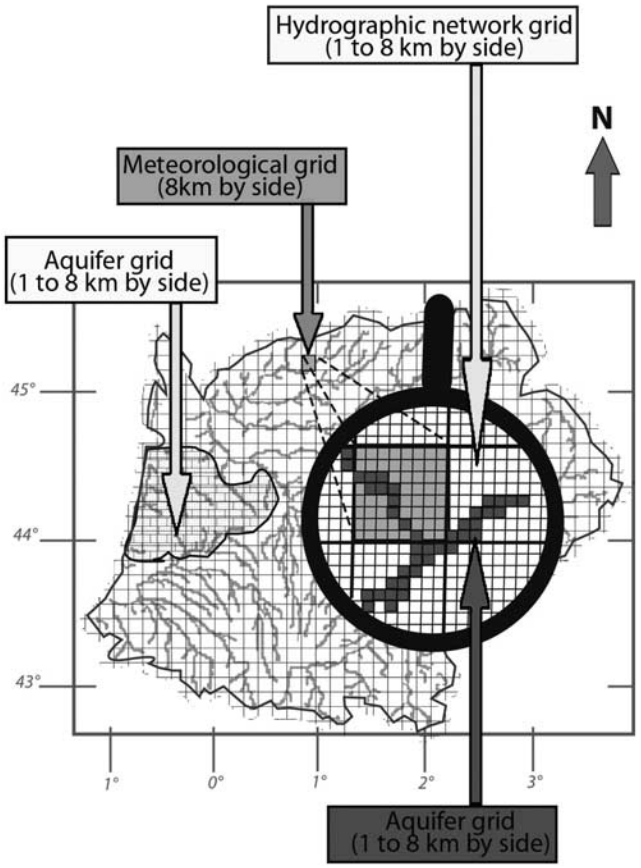

Figure 3. Organization of the different grids used for modeling the meteorological forcing, the superficial hydrographic network, and the aquifer extension.

measurement campaigns [*Mahfouf and Noilhan*, 1996; *Boone et al.*, 1999]. Various recent parameterizations have improved the hydrological processes, mainly: a subgrid parameterization for the runoff and the deep drainage [*Habets et al.*, 1999a], a soil freezing scheme [*Boone et al.*, 2000], and a three-layer scheme for explicitly modeling snow cover [*Boone and Etchevers*, 2001]. The surface runoff and the drainage flux calculated by ISBA for each grid cell are transferred at the daily time step to the macroscale hydrological MODCOU model surface and underground networks.

[10] MODCOU computes the ground water evolution and the river flow. The latter is estimated by routing the water from each grid cell of the river basin to the river cells and from the river cells to the outlet using isochrones. The evolution of the water table head is simulated using the diffusivity equation. In this study, there was no simulation of the feedback from the water table to the near-surface vadose zone. The water flux from the ground water table to the river is computed using a simple relationship between the water level head and the altitude of the river cell. The model resolution varies from 1 to 8 km, allowing a fine description of the drainage network and thus the simulation of the daily discharges at any hydrometric station within the river basin.

2.2.2. Modeling Method

[11] The hydrological behavior of the Adour-Garonne river basin was simulated at a daily time step for the 10 hydrological years of the 1985–1995 decade (assuming that a hydrological year begins in August and ends in July). This model configuration was based on the work done by *Voirin-Morel* [2003], who first applied the SIM system to this region for the same time period. The dense basin hydrographic network has been discretized using grid cells of varying spatial resolution depending on the complexity of the network (Figure 3). The physiographic parameters needed by ISBA (the soil texture, the vegetation type, the leaf area index distribution, the vegetation fraction, the albedo and the surface roughness) were obtained from the ECOCLIMAP [*Masson et al.*, 2003] database, which merges information from vegetation maps, climate zones and satellite data. The soil texture, represented by the fraction of sand and clay, is obtained from the French Institute of Agronomy (INRA) at a spatial resolution of 1 km. The vegetation parameters were extracted from the SPOT/VEGETATION satellite sensor and were used to derive the changes in the vegetation at 10-day increments. The atmospheric forcing was computed by SAFRAN for each of the 1758 8-km cells of the meteorological grid (Figure 3) at a 3-hour time step for the 1985–1995 period. Using this forcing together with the physiographic parameters, the different terms of the hydrological budget (evaporation, runoff and infiltration) were simulated by ISBA for each cell of the meteorological grid. The simulated outgoing water fluxes (surface runoff and deep drainage) were transferred to the 40,248 superficial hydrographic network grid cells (Figure 3), with only the deep drainage feeding the 2,861 grid cells of the Landes aquifer. Therefore the small aquifers along the main rivers were not explicitly taken into account by the hydrological model. MODCOU computed the water transfer to and within the river, thereby simulating the river discharges at the 81 available hydrometric stations [*Voirin-Morel*, 2003]. Among these hydrometric stations, 16 were chosen for the present study and called the reference stations. They were selected for an analysis of the climate change impact both on the main basins and on the different climatic subregions of the study zone.

[12] A key aspect of this study is that the analysis is based on "naturalized" river flow. Since irrigation is not insignificant in the Adour-Garonne basin, mainly because of maize production, the natural river flow is modified by dams and the channel supply is used to sustain irrigation. The naturalized river flow is based on daily observed discharges that were corrected for the influence of human activities (water storage, transfer by channels for irrigation, etc.). These corrections were made using data provided by the Adour-Garonne water agency. Human activity is taken into account at a daily timescale by adding the amount of water corresponding to a withdrawal (inflow) of water in the river due to a channel supply (drainage) or a reservoir filling (emptying) to the discharge. It is essential to use the resulting naturalized river flows to be able to study the climate change impact without taking into account any hypothesis on the changes in human activity.

2.2.3. Low-Flow Period

[13] The low-flow period is of special interest in the Adour Garonne basin, since the availability of water is low while the demand is large, particularly because of irrigation. During this period, the river flow is already

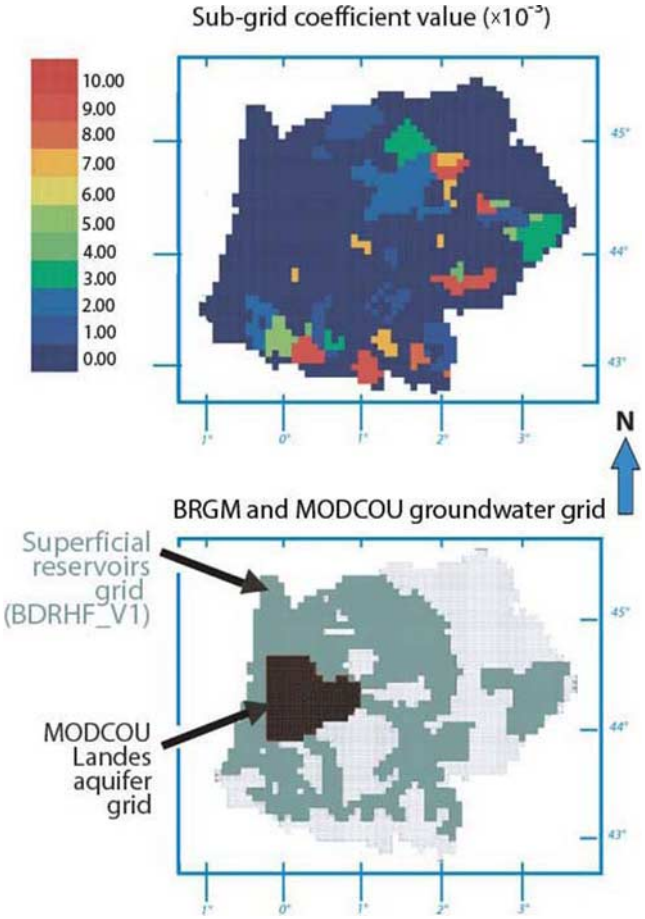

Figure 4. Spatial distribution of the subgrid drainage coefficient value (unit: m^3/m^3) for the superficial reservoir grid cells.

below its critical value almost every year, which results in water use restrictions and generally poor water quality. Estimating the climate change impact on the river discharge during the low-flow period is essential, and requires an understanding of how the surface water and the groundwater contribution will be affected by the climate change.

[14] Despite the satisfying modeling results obtained at the 81 hydrometric stations [*Voirin-Morel*, 2003], the ISBA subgrid drainage parameterization was modified in order to improve the simulation during the low-flow period. Subgrid drainage parameterization allows the SIM model to take into account the effect of alluvial aquifers and natural perched groundwater reservoirs (hereinafter called superficial reservoirs) that contribute to sustaining the river flow during low-flow periods. In ISBA, the drainage is simulated restoring the soil water content to the field capacity, which represents equilibrium between the gravitational and capillarity forces. However, during the summer period the soil water content is generally lower than field capacity. At this point, in order to represent the unresolved alluvial and perched aquifers, the so-called subgrid drainage [*Habets et al.*, 1999a] production mechanism is activated. It produces a constant minimum base flow which sustains a minimal river discharge. For the soil water content below field capacity, the subgrid drainage mechanism is considered as constant and dries the soil at a rate depending on the coefficient (W_{drain}). The value is generally set to 10^{-3} m^3/m^3 for all the cells of the ISBA grid covering the study area [*Habets et al.*, 1999b; *Etchevers et al.*, 2002]. In the present study, W_{drain} was calculated only for the cells where superficial reservoirs were identified using the French Geological Survey (BRGM) groundwater database (BDRHF, http://sandre.eaufrance.fr); it was set to 0 elsewhere in order to improve the simulation results during the low-flow periods.

[15] W_{drain} was estimated using the following methodology: For each of the monitored subbasins, a characteristic discharge (Q_c) was defined as the mean of the 1200 lowest daily discharges in the 1985–1995 period. Q_c was considered to be representative of the mean daily discharge for the 4-month low-flow period (4 × 30 days × 10 years = 1200 days) during the 1985–1995 decade. In this approach, it is assumed that low discharge occurred over 4 months and that the discharge in all other months was larger. This assumption does not introduce a significant underestimation of the characteristic discharge due to the relative quality of the low-flow period discharge data (the influence of dams and irrigation were accounted for).

[16] The Q_c of a given monitored subbasin (Q_{cM}) can be calculated from equation (1) as

$$Q_{cM} = W_{drainM} \times \frac{A_{cell}}{T_o} \times \sum_i (C_{3i} \times D_{3i} \times A_i) \qquad (1)$$

where A_{cell} is the area of an ISBA grid cell (8 km × 8 km), T_o is 86,400 s, C_{3i} is a force-restore coefficient which controls the drainage intensity [*Mahfouf and Noilhan*, 1996; *Boone et al.*, 1999), D_{3i} is the soil depth and A_i is the fractional area of the grid cell contained in the monitored subbasin. With this equation, one W_{drainM} value was calculated and applied to all of the grid cells containing superficial reservoirs within the given monitored subbasin.

[17] The calculation of the W_{drain} values was made from small to large subbasins. Consequently, the Q_c of a downstream subbasin (Q_{cD}) containing one or more smaller upstream subbasins was calculated including the corresponding Q_{cU} values:

$$Q_{cD} = Q_{cU} + W_{drainD} \times \frac{A_{cell}}{T_o} \times \sum_j (C_{3j} \times D_{3j} \times A_j) \qquad (2)$$

The resulting W_{drainD} value was applied only to the grid cells j located outside the incorporated upstream subbasins.

[18] Figure 4 presents the spatial distribution of the coefficient values over the basin. W_{drain} values ranged from 0 to 10^{-3} m^3/m^3 and they were set to 0 over the Landes aquifer (since the groundwater processes are simulated by MODCOU). This method is more an estimation than a calibration (in the classical sense) as there was no optimization procedure to fit the observed values using efficiency criteria. However, it provided a robust way to obtain a map of W_{drain} values depending only on predefined ISBA parameters and observed river flow.

[19] This map was then validated by comparing the simulated daily discharges to the observed data using efficiency criteria (for example, see Figure 5) over the entire 1985–1995 period. Figure 5 shows how the simulation results were improved when including the deep drainage

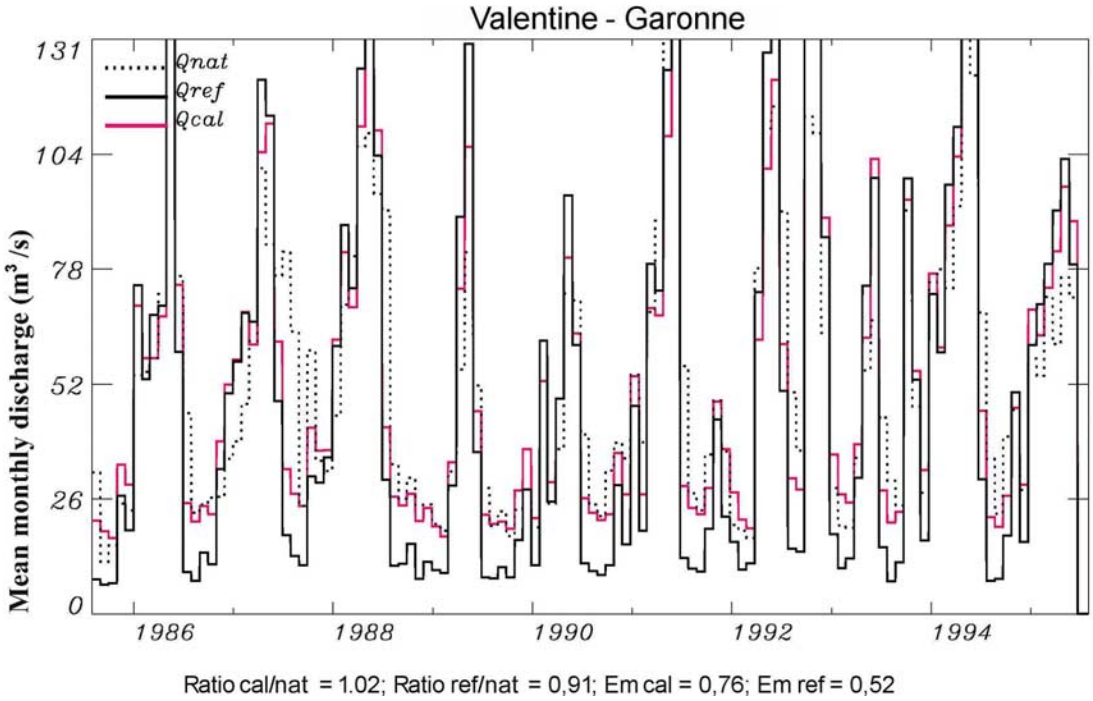

Figure 5. Mean monthly river discharges at the Valentine hydrometric reference station for the Garonne River: Q nat: observed values corrected for irrigation and hydropower activity influences; Q ref: simulated without low-flow adaptation; Q cal: simulated values after low-flow adaptation. The statistical criterion ratio (ratio of the simulated mean monthly river discharge to the observed river discharge) and Em (Efficiency or Nash criterion defined on a monthly basis [*Nash and Sutcliffe*, 1970]) show the simulation quality improvement after the low-flow adaptation.

adaptation for the Valentine station located on the Garonne River. The statistical criteria used to evaluate the model's accuracy show both the relatively good agreement between the simulation and the discharge observed. The statistical criteria values calculated after incorporating the deep drainage adaptation for the 16 other reference hydrometric stations are summarized in Table 1. They show the generally good simulation results despite the meteorological, geomorphological and hydrogeological heterogeneity of the domain studied. These results validated the present hydrometeorological model for the Adour-Garonne basin, making it possible to study the climatic change impact on the water resources.

3. Impact of the Simulated Climate Changes on the Water Resources of the Adour-Garonne Basin

3.1. Climate Change Simulations

[20] Predicting the water resources under climate change at a regional scale implies that the problems of spatial variability and uncertainties in both climate predictions and hydrological modeling must be addressed [*Leung and Wigmosta*, 1999]. Various sources of uncertainty are related to the future climate simulation. The major sources of uncertainty, considered in descending order, are the emission scenarios [*Arnell et al.*, 2004], climate model parameterization (particularly for precipitation), downscaling [*Boé et al.*, 2006] and finally the hydrological model parameterization [*Etchevers et al.*, 2002; E. Leblois and J. M. Gresillon (Eds.), GICC-Rhône, 2005, available at http://medias.obs-mip.fr/gicc/interface/projet.php?2%2F00]. In the present study, only the uncertainties related to climate model parameterizations were considered. The hydrological responses of the SIM system were explored in an off-line mode using time slice and continuous climate-forcing data sets from four European state-of-the-art GCMs. All of the GCMs used in the B2 greenhouse gas scenario were defined by the Special Report on Emission Scenarios (SRES); [*Houghton et al.*, 2001]. The time slice simulations were taken from a previous study by *Polcher et al.* [1998] using the Laboratoire de Météorologie Dynamique (LMD), the CNRM (Centre National de Recherches Météorologiques (LMD), the Hadley Centre (HC) and the University of Reading (UR) GCM models. Note that the CNRM and LMD models contributed both relatively low resolution (LR: about 200 × 400 km on the Adour-Garonne basin) and high resolution (HR: from 50 × 50 to 100 × 100 km on the Adour-Garonne basin) precipitation and temperature fields (see Table 2 for GCM details). The GCM simulations were performed over 30 years for two periods: one with the present greenhouse gas concentration (1 × CO_2: representing present climate conditions for 1985–1995), and the other with 2 × CO_2, which represents the future climate conditions (for the decade 2050–2060). On the basis of these simulations, monthly averaged values were calculated for the precipitation and the lowest model level atmospheric temperatures: The differences between the present and future decades were then used to calculate anomalies.

[21] The precipitation and temperature fields simulated by the climate version of the ARPEGE/IFS coupled ocean-atmospheric model simulation [*Gibelin and Déqué*, 2003]

Table 1. Statistical Criteria Calculated for the 16 Reference Stations to Analyze the Daily Simulation Results for the 1985–1995 Period[a]

Reference Stations, River	Ratio, Q Calibrated (Qcal)/Q Observed (Qnat)	Em
Foix, Ariège	0.85	0.72
Auterive, Ariège	0.93	0.80
Valentine, Garonne	1.02	0.76
Roquefort, Salat	0.77	0.78
Portet, Garonne	0.91	0.85
Lamagistère, Garonne	0.88	0.89
Tonneins, Garonne	0.92	0.89
Villemur, Tarn	0.82	0.82
Loubejac, Aveyron	1.02	0.86
Estirac, Adour	1.06	0.62
Aire, Adour	1.05	0.79
Audon, Adour	1.06	0.81
St Vincent, Adour	1.00	0.91
Escos, Gave d'Oloron	0.81	0.81
Berenx, Gave de Pau	0.94	0.79
Bergerac, Dordoge	0.88	0.87

[a]Ratio represents the ratio of the simulated to the observed mean monthly river discharges; Em (Efficiency) is the Nash criterion (estimator defined as one minus the sum of the absolute squared differences between the simulated and observed values normalized by the variance of the observed values during the period under investigation [*Nash and Sutcliffe*, 1970]).

covering the period 1961–2100 at a maximum resolution of 0.5° (~50 km) over the Mediterranean region, were used as a seventh scenario over the period 1985–2100 (see Table 2). For this transitory simulation, the anomalies were computed over 10-year periods in order to examine the simulated climate trend over the 21st century.

[22] One of the key aspects of the climate change impact study is the spatial and temporal downscaling of the GCM results. In this study, the downscaling technique, called the alteration method (the fourth method described by *Xu* [1999]), was used. In this method, the generation of climate scenarios consists in (1) estimating average annual changes in temperature (δT) and precipitation (δP) using the GCM results and (2) adjusting the historic temperature and precipitation series using these values (see section 0 below). This simple method allows the modeller to eliminate the biases due to the climate simulation (differences between observed and simulated climate) in terms of the hydrometeorological forcing. It was used in several studies for French watersheds to obtain the high-resolution forcing data required for the hydrometeorological models (GICC-Rhône experiment [*Noilhan et al.*, 2001; *Etchevers et al.*, 2002]). It integrates the climate change signal simulated by the GCM into the atmospheric forcing applied to the SIM system while retaining the relatively high spatial and temporal resolution of the present-day forcing data. However, it should be noted that the modifications that occur at finer spatial and temporal scales (concerning dry and wet spells, daily extreme events, changes in spatial and temporal correlation of climatological variables or numbers of dry and wet days) are not captured.

3.2. Present Climate Simulation

[23] In order to examine to what extent the GCMs were able to catch the main characteristics of the domain under study, the simulated mean monthly temperature and precipitation values were compared to the mean monthly values observed for the 1985–1995 decade (Figure 6). All of the models' simulated annual cycles are generally in good agreement with the observed trend, except for the LMD and the CNRM models, which overestimate the temperatures in summer and over the whole year, respectively. The precipitation simulations vary more depending on the model considered. They are globally better simulated in winter than in summer, when they are generally underestimated. Besides the LMD-HR model case, it appears that the models with the relatively high spatial resolution simulate both the regional temperature and precipitation better than the low-spatial-resolution models.

3.3. Climate Anomaly Construction

[24] The monthly precipitation and temperature (δTa and δP) anomalies were calculated (equations (3) and (4)) in order to modify the present (1985–1995) observed atmospheric forcing. A positive temperature or precipitation anomaly value means an increase in the variable for the 2050–2060 decade ($2 \times CO_2$) relative to the present ($1 \times CO_2$). Since the fields simulated by the continuous ARPEGE scenario were available for only two decades, the anomalies were computed from

$$\delta \mathrm{Ta} = \mathrm{Ta}_{2\times \mathrm{CO}_2} - \mathrm{Ta}_{1\times \mathrm{CO}_2} \tag{3}$$

$$\delta \mathrm{P} = \frac{\mathrm{P}_{2\times \mathrm{CO}_2} - \mathrm{P}_{1\times \mathrm{CO}_2}}{\mathrm{P}_{1\times \mathrm{CO}_2}} \tag{4}$$

Figure 7 presents the basin's averaged mean monthly temperature and precipitation anomalies for the seven GCMs. The anomaly values are of the same order as that obtained for the Rhone study, which was done with all but the ARPEGE/IFS coupled ocean-atmospheric model's [*Gibelin and Déqué*, 2003] continuous scenario [*Noilhan et al.*, 2001]. The temperature anomalies are generally positive and more intense in the summer (3–4 degrees) than

Table 2. Spatial Resolution of the Global Climate Models Used Over the Adour-Garonne Basin

Research Institute and Abbreviation	Spatial Resolution
Low-Resolution Models	
Hadley Centre, England (HC)	2.5° × 3.5°, 137 × 388 km
Laboratoire de Météorologie Dynamique, France (LMD_LR)	1.6° × 3.75°, 88 × 416 km
University of Reading, England (UR)	2.8° × 2.8°, 154 × 310 km
Centre National de Recherche Météorologiques, France (CNRM_LR)	3.8° × 3.7°, 209 × 410 km
High-Resolution Models	
Laboratoire de Météorologie Dynamique, France (LMD_HR)	100 km
Centre National de Recherche Météorologiques, France (CNRM_HR)	50 km
Centre National de Recherche Météorologiques, France (CNRM_continuous)	60 km

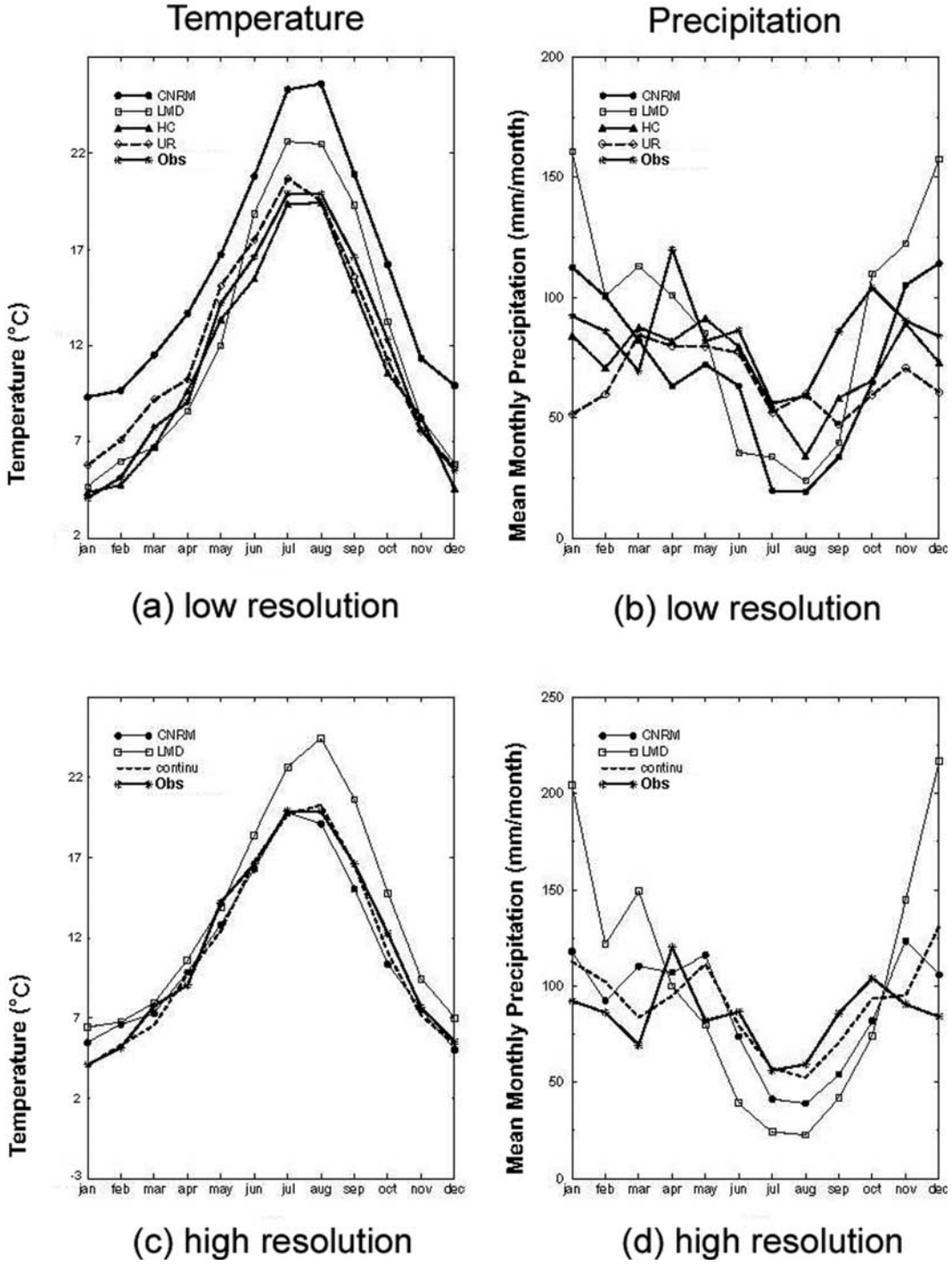

Figure 6. Comparison of the different global climate models (GCMs) on monthly simulated and observed (Obs) temperature and precipitation averaged over the region studied, for the 1985–1995 period over the Adour-Garonne river basin (modified from *Lehenaff* [2002]). (a and b) Low-spatial-resolution models. (c and d) High-spatial-resolution models; "continu" represents the CNRM continuous scenario.

in the winter (1–2 degrees). The Hadley Centre model predicts a very significant temperature anomaly, on the order of 9 degrees in August, which is even greater than that calculated for the Rhône River basin (approximately 8 degrees [*Noilhan et al.*, 2001]). The precipitation anomalies are generally positive during the winter and negative in the summertime (especially for the high-resolution GCMs). The anomalies for some months exceed the simulated present climate values by 50%. This general tendency is less clear for the precipitation anomalies calculated from the low-resolution GCMs, where, for instance, the LMD scenario predicted an increase in precipitation in spring and a deficit for the rest of the year.

3.4. Climate Scenarios

[25] The 2050–2060 temperature and precipitation forcing data were calculated by applying the monthly anomalies

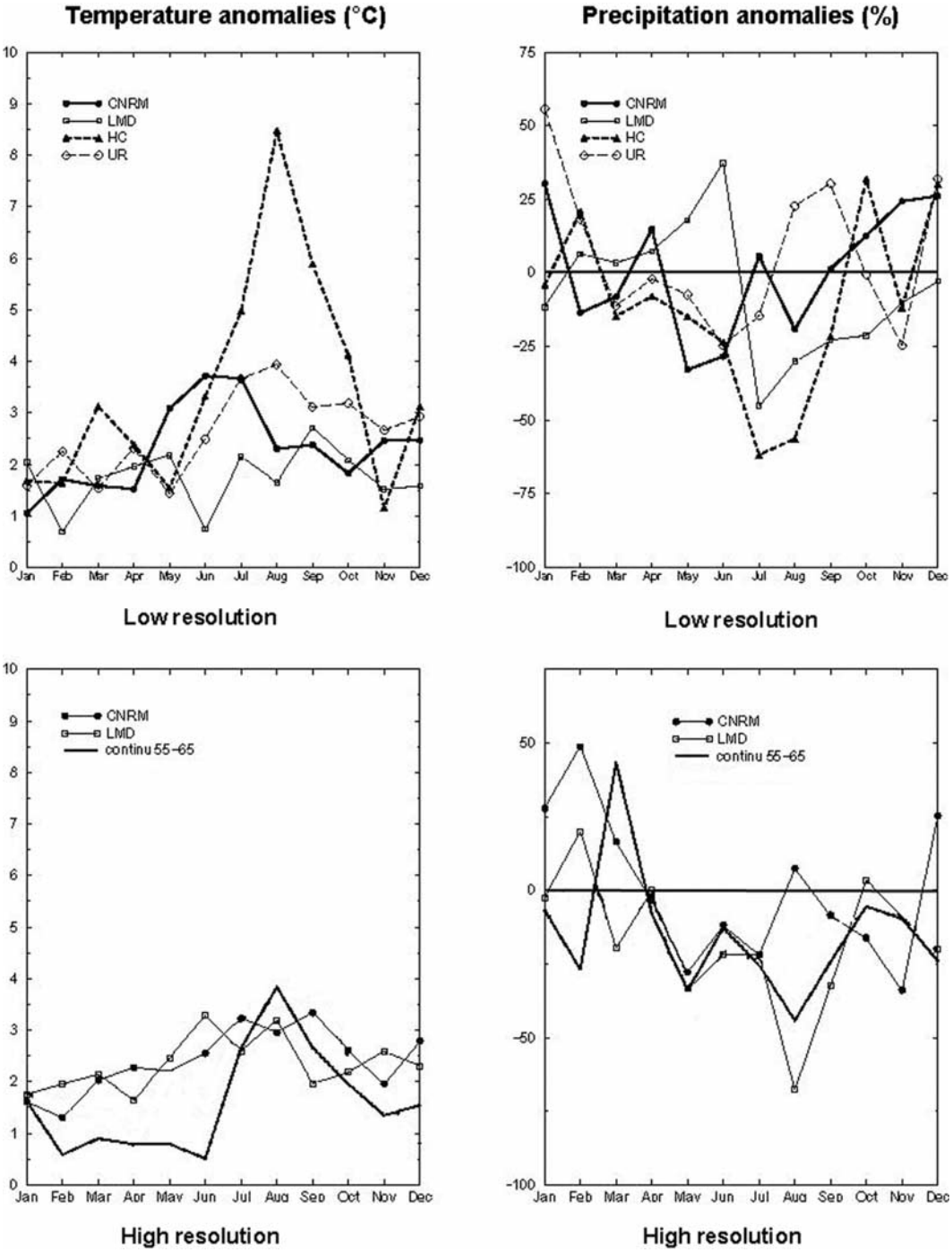

Figure 7. Monthly temperature and precipitation anomalies calculated from the seven GCM outputs for the present (1985–1995) and the modified climate (2050–2060) averaged over the region studied (modified from *Lehenaff* [2002]). The Action Recherche Petite Echelle et Grande Echelle (ARPEGE) continuous scenario anomalies are available for the 2055–2065 decade.

to the present values observed and analyzed by SAFRAN (equations (5) and (6), where T_{mc}, T_{pc}, P_{mc} and P_{pc} are the 3-hour time step temperature and precipitation values for the modified climate and the present climate, respectively).

$$T_{mc} = T_{pc} + \delta T_a \tag{5}$$

$$P_{mc} = P_{pc} \times (1 + \delta P) \tag{6}$$

[26] This resulted in seven so-called climate scenario (six time slice and one continuous) forcing data sets for the 2050–2060 hydrological simulation (integrating precipitation and temperature change simulated by the four GCMs at high and low resolutions). Modifying the precipitation and the temperature affects the surface soil/vegetation tempera-

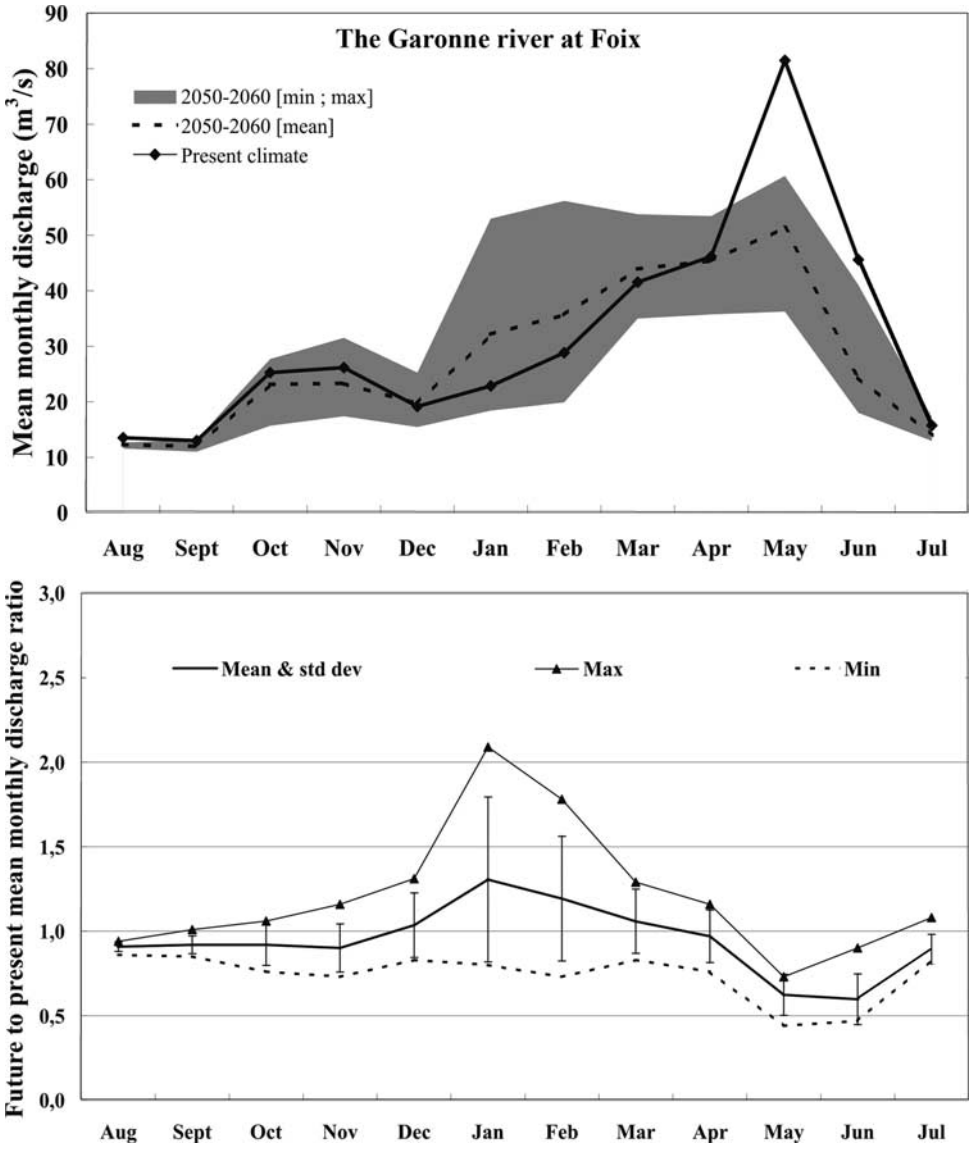

Figure 8. (top) Mean monthly discharges simulated at the Foix hydrometric station for the present decade (1985–1995) and the future decade (2050–2060, mean value and envelope curve containing the mean monthly discharge values simulated in the seven scenarios and limited by the extreme values for each month). (bottom) Ratios of the mean monthly discharges simulated under the climate scenarios to the mean monthly discharges simulated under the present climate (mean monthly value along with the standard deviation range and extreme values for each month).

ture and the volumetric water content. This in turn modifies the evapotranspiration computation, as only one energy balance is considered in ISBA for the entire soil-vegetation system [*Noilhan and Mahfouf*, 1996].

4. Discussion of the Simulation Results for the 2050–2060 Period

[27] The hydrological response of the basin to the modified climate scenarios was analyzed by comparing the future and present-day simulated river discharges at the hydrometric stations. For this analysis, it is assumed that there is no spatial and temporal climatic variability of the surface parameters such as vegetation cover and type, land use and climatic regime (only the intensity of the monthly values of temperature and precipitation are modified compared with the 10-year SAFRAN analysis).

4.1. Seasonal Impacts on the River Discharges

[28] The mean daily simulated river flows in each climate scenario at the main hydrometric stations were averaged to obtain mean monthly values over the entire 2050–2060 period. The comparison was made by computing the ratios between the future (2050–2060 decade) and the present (1985–1995 decade) mean monthly simulated discharges. In order to analyze the seasonal variability of the impacts, only the mean results of the seven scenarios and the corresponding standard deviations were plotted together with the mean monthly simulated values of the present climate (example in Figure 8, top). The impact of each scenario can be assessed by the ratio between the present

and the future simulation: There is an increase in the mean monthly river discharge when its value is greater than 1 and a decrease when its value is less than 1 (example in Figure 8, bottom). The scenario's variability is assessed by the envelope on the basis of the monthly standard deviation. The shape of the envelope shows the amplitude of the variability between the scenarios (see Figure 8). Instead of comparing simulated future river flow to the observed present-day values, the future discharges (2050–2060 decade) were compared to the simulated present discharge (1985–1995 decade) in order to minimize the errors related to the hydrological simulation. Moreover, this allows an estimation of the impact of the differences between the seven modified climate scenarios. The results are presented on a seasonal basis, and special attention is paid to the evaluation of the impacts during the low-flow period (July–October). Only the results at selected stations are presented in this paper in order to show the typical impacts on the main aspects of the river basin under consideration, which are processes related to the mountains and the plains with and without significant aquifer catchments), but the results for all of the 16 hydrometric stations are available in *Caballero and Noilhan* [2003].

4.1.1. Geographical and Seasonal Variability of the Impacts

[29] First, it can be observed that there is significant variability of the climate scenario impacts depending on the geographical context of the catchments considered. For the mountainous catchments (e.g., the site located on the upper part of the Ariège River monitored at the Foix River gauge: the highest station, 400 m asl; Figure 1), the impacts of the climate scenarios are the most significant in the winter and the spring, but there is more variability in winter than in spring (Figure 8). All of the scenarios bring about a decrease in the simulated discharge in spring and summer. The mean impact of the scenarios results in a discharge decrease in autumn and an increase in winter, but this is not the case for all of the scenarios. The decrease in autumn is related both to the simulated precipitation deficit and the highest annual simulated temperatures, particularly those predicted by the high-resolution models. Moreover, as the soil is drier at the end of summertime, it takes a longer time to moisten, thereby reducing the fraction of the fallen precipitation that feeds the river. The discharge increase in winter is due to the higher rainfall (positive anomalies leading to more precipitation during this season and higher temperatures increasing the liquid precipitation ratio; see Figure 7) and the lower snow cover storage. Impact on the snowpack is significant, which is described in section 4.1.2. The impact on the snowpack plays an important role on the river flow: As the snowmelt began earlier, the snow cover was reduced in spring, so that the river discharge was reduced in spring by nearly 50% for certain extreme scenarios. This might have a large impact for the recharge of the reservoirs located in the mountains, which are usually filled by the snowmelt. Consequently, the low-flow period starts earlier, which explains why the mean river discharge decrease is higher in July than in October and lasts longer than for the present period.

[30] Looking at the climate scenario impacts downstream of the Garonne River reveals how, as the surface area of the river basin increases and its mean altitude decreases, the snow cover influence on the river flow regime decreases. The Tonneins River gauge is the lowest of the Garonne River basin stations (38 m asl.; Figure 1). As can be seen in Figure 9, the large discharge decrease observed at the Foix station in spring is smaller at the Tonneins station. The LMD low-resolution scenario results in a small increase in June, certainly related to the precipitation increase simulated by this model for that period; see Figure 7 (the coarse resolution of this model did not lead to substantial differences in space between the precipitation anomalies in the different regions of the study and the basin's average anomalies). Moreover, the extreme winter discharge ratio at Tonneins barely exceeds 1.5 while it reaches 2 at the Foix station, because the drainage area of the Garonne in Tonneins encompasses watersheds where rainfall dominates, while the Ariège at Foix drains a basin dominated by snowmelt. At Foix, the discharge increase in winter and decrease in spring are caused by the precipitation and temperature increases which lead to the snow cover storage reduction and to an earlier melt. At Tonneins, the temperature increase has a lesser impact because of the mean altitude of the watershed and so the winter river discharge increase is only related to the precipitation increase. These differences in the impact of the climate scenario between Foix and Tonneins have been observed at all of the hydrometric gauges along the Garonne River and also along the other rivers of the Adour-Garonne basin [*Caballero and Noilhan*, 2003].

4.1.2. Impacts on the Snow Cover

[31] *Etchevers et al.* [2002] and *Voirin-Morel* [2003] have shown that the SIM system is able to accurately reproduce the actual snowpack changes compared to the observations at ski resorts in the French Pyrenees and Alps mountain ranges. In the present study, the same system is used to study the impact of the climate change on the snowpack. The impact of the simulated climate change on the snow cover is found to be very intense and to significantly influence the river flow regime for the mountainous basins, as was discussed in section 4.1.1. The increased temperature simulated by the GCMs leads to a decrease in the winter's solid precipitation and a corresponding increase in liquid precipitation. Figure 10 presents the impact on the snow cover depth and duration simulated by ISBA at six Pyrenean observation sites, using the continuous scenario. It can be observed that the snowpack greatly decreases between the present time and the end of the century. This decrease, while nonlinear, provokes a reduction of the snow cover depth and duration for the 2050–2060 decade in comparison with the present state, ranging between roughly 30% and 20% at the low-altitude mountain site, to between 20% and 10% at the high-altitude mountain site. This reduction results in an earlier snowmelt compared with the present state and is therefore responsible for the future simulated river discharge decrease in spring, as seen at, for instance, the Foix River gauge (Figure 8).

4.1.3. Impacts on the Low-Flow Period

[32] The climate scenario impact on the low-flow period was analyzed and the following general conclusions on the tendencies for the whole basin were drawn.

[33] Table 3 presents a synthesis of the impacts on the river discharges. The mean and the minimum monthly discharge ratios (Ri) are calculated following the equation (7), where

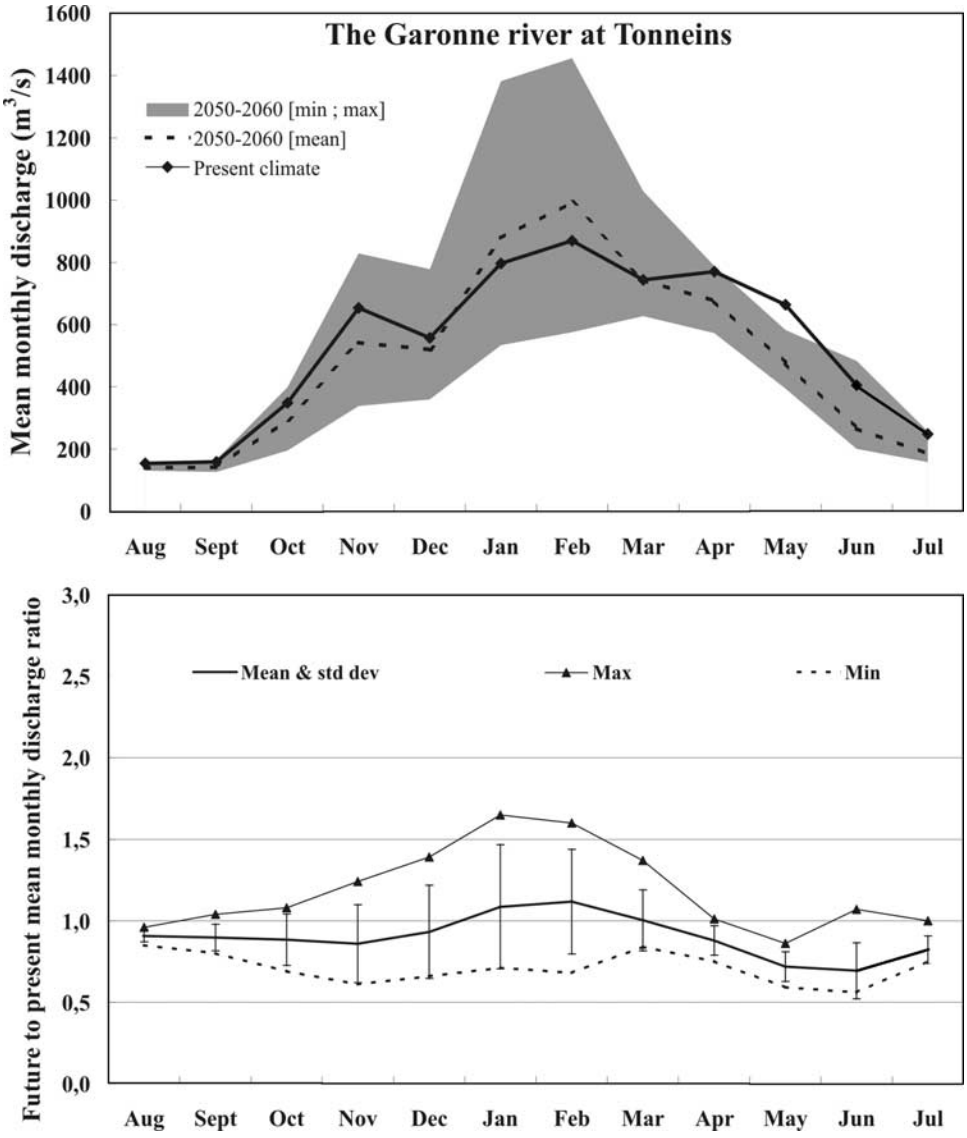

Figure 9. As in Figure 8, except for the Tonneins hydrometric station.

Q_{i-mc} is the mean or the minimum monthly discharge simulated under modified climate and Q_{i-pc} is the mean or the minimum monthly discharge simulated under the present climate.

$$R_i = \frac{Q_{i-mc}}{Q_{i-pc}} \quad (7)$$

[34] For each hydrometric station, the simulated discharges for each climate scenario were averaged over the 4-month low-flow period. This was done to estimate the mean and the extreme impacts of the scenarios for this period. The standard deviation is also given to illustrate the variability of the impacts of each scenario. The overall impact of the seven scenarios is an approximately 11% decrease in the low-flow period river discharges for all of the hydrometric stations. The mean standard deviation for all scenarios is 0.08. This indicates that, despite the variability between the different scenarios, the trend toward a river discharge decrease is relatively strong for the low-flow period. The stronger impacts can be observed in July, for which the mean monthly simulated discharge decreases by 15% on average. However, the variability between the different scenarios is higher in October than in July. Consequently, some scenarios can lead to a higher decrease in October than in July, which can even exceed 20%. The impact on the minimum mean monthly simulated discharges (corresponding to an 8% decrease on average) is lower than the impact on the mean discharges. These last two observations can be explained by the fact that the base flow that sustains most of the river flow in summertime is strongly driven by the climate (i.e., mainly by precipitation) in winter and spring, and is therefore less sensitive to the climate change in summer. This result suggests that the base flow presents a lower sensitivity than the overland flow to the climate scenarios. It can thus be suggested that the end of the low-flow period (and the lowest discharge) will be less sensitive to the simulated climate change than the beginning of the low-flow period and the flows for the rest of the year. However, this relative lower sensitivity is

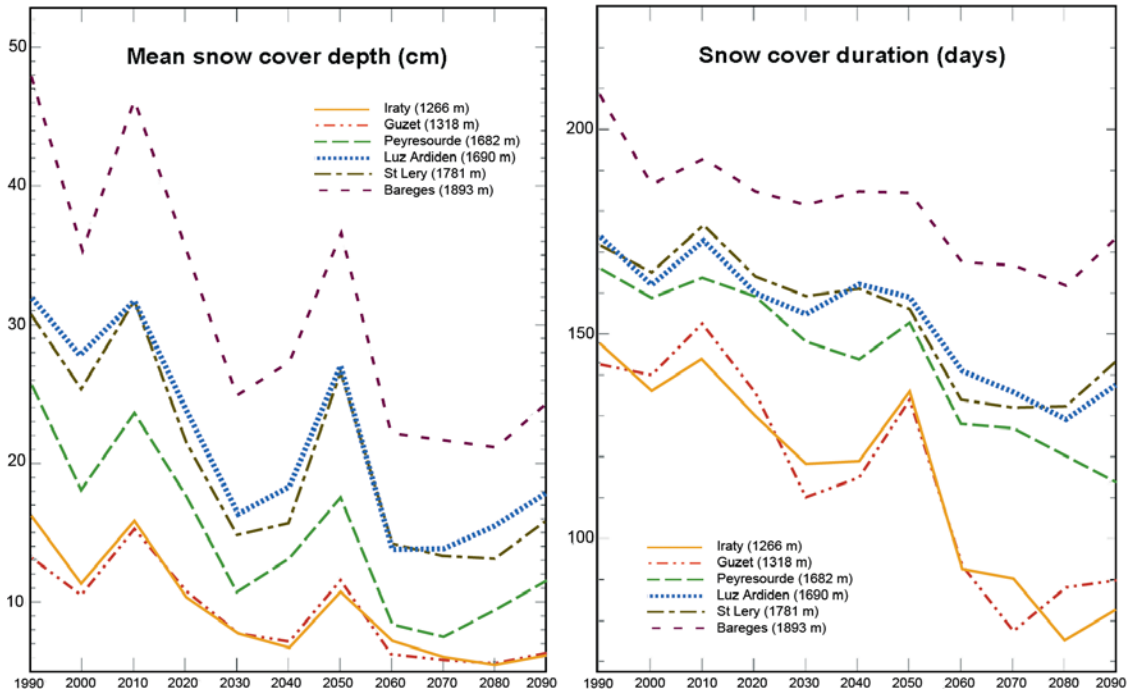

Figure 10. Evolution of the mean snow cover depth (in cm) and duration (in days) simulated for six mountain stations located between 1266 and 1893 m asl, under the continuous climate scenario based on the ARPEGE/IFS coupled ocean-atmospheric model simulation [*Gibelin and Déqué*, 2003], between 1990 and 2090 (modified from *Lehenaff* [2002]).

strongly dependent on the winter recharge and can be increased for the case of a deficit in the winter precipitation, as will be shown in section 4.1.4.

[35] The climate scenario impacts for the low-flow period are roughly of the same order at all of the stations along the river, while their variability slightly increases downstream. Nevertheless, the climate scenario impacts on the catchments containing significant groundwater systems are slightly different from those presented for the Garonne basin. In the Adour basin (Figure 1) for example, which contains a part of the large Landes aquifer, it can be observed that the climate scenario impacts and their variability throughout the year at the St Vincent stream gauge are moderate in comparison to the other river gauges (Figure 11). This is probably due to the Landes aquifer, which has a contribution which is known to sustain the streamflow in the summertime [*Habets et al.*, 1999c]. The higher winter precipitation of the climate scenarios may enhance this phenomenon, reducing the decrease of the summer river flow in comparison to the other basins. The influence of the Landes aquifer must, however, be tempered by the fact that the spatial variability of the climate scenarios could explain part of the results. The Landes aquifer contribution to the base flow discharge nevertheless plays an important role, as can be seen when comparing the mean simulated discharges during the low-flow period, which are higher at the St Vincent station than at the upstream stations of the Adour River basin (Table 3).

4.1.4. Impacts on the Low-Flow Period for Two Extreme Situations

[36] To examine the impact on the low-flow period under extreme situations, the river flows simulated for the wettest year and for the driest year were examined. The average discharge from July to October of the driest year in future climate conditions was compared to that simulated under the present-day climate: The same was done for the wettest year. This provided an estimation of the minimum and maximum impacts that could occur during the low-flow period in the future. The driest year of the present decade was the hydrological year 1988–1989, where the total rainfall was 740 mm. The wettest year was 1993–1994 with a total rainfall of 1310 mm. The driest and wettest years mainly differ in terms of the amount of winter rainfall (the summer rainfall totals are only slightly different). The future climates for the driest and wettest years were calculated by applying the seven precipitation and temperature anomalies to the meteorological data of both of the extreme years. The simulated mean and standard deviations of the future monthly discharges during the low-flow period obtained for each year are compared in Table 4.

[37] The results show that the mean simulated discharge decrease during the low-flow period is stronger for the wet year than for the dry year, with a difference close to 5% on average. The same is observed for the variability of the hydrological responses to the different scenarios, where the wettest year's standard deviation is three times greater than that for the driest year. Moreover, it can be observed that the low flows mean a discharge ratio decrease over all of the hydrometric stations for the dry year is of the same order as the one obtained over the whole decade: 11%. This is probably related to the amount of soil water content, which must be lower for a dry year than for a wet year at the beginning of the low-flow period. Generally speaking, the climate scenario simulated by all of the models can be

Table 3. Mean, Standard Deviation, Minimum and Maximum Values of the Simulated Discharge Ratios Between the 2050–2060 and the Present Decade Under All Scenarios[a]

Hydrometric Stations	Types of Value	Jul	Aug	Sep	Oct	Low Flow (Jul–Oct)	Minimal Discharge
Foix, Ariège	Mean	0.89	0.91	0.92	0.92	0.91	0.92
	SD	0.09	0.03	0.05	0.12	0.06	0.03
	Min	0.83	0.86	0.85	0.76	0.82	0.86
	Max	1.08	0.94	1.01	1.06	0.99	0.96
Auterive, Ariège	Mean	0.89	0.91	0.92	0.92	0.91	0.91
	SD	0.09	0.03	0.06	0.12	0.06	0.03
	Min	0.82	0.86	0.85	0.75	0.82	0.86
	Max	1.09	0.94	1.02	1.07	0.99	0.95
Valentine, Garonne	Mean	0.78	0.87	0.87	0.88	0.85	0.87
	SD	0.10	0.05	0.09	0.15	0.07	0.06
	Min	0.69	0.79	0.75	0.71	0.73	0.76
	Max	0.99	0.92	1.04	1.12	0.97	0.96
Roquefort, Salat	Mean	0.87	0.91	0.91	0.90	0.90	0.91
	SD	0.11	0.03	0.05	0.12	0.06	0.03
	Min	0.79	0.85	0.84	0.76	0.81	0.86
	Max	1.11	0.93	1.01	1.09	0.99	0.96
Portet, Garonne	Mean	0.83	0.89	0.89	0.89	0.88	0.90
	SD	0.10	0.03	0.07	0.14	0.07	0.05
	Min	0.75	0.83	0.80	0.73	0.78	0.82
	Max	1.04	0.92	1.03	1.10	0.99	0.96
Lamagistère, Garonne	Mean	0.83	0.90	0.90	0.88	0.87	0.90
	SD	0.09	0.03	0.07	0.15	0.07	0.05
	Min	0.75	0.85	0.80	0.69	0.76	0.83
	Max	1.02	0.94	1.02	1.07	0.98	0.97
Tonneins, Garonne	Mean	0.82	0.91	0.90	0.88	0.87	0.91
	SD	0.08	0.04	0.08	0.16	0.08	0.05
	Min	0.75	0.85	0.80	0.69	0.76	0.84
	Max	1.00	0.96	1.04	1.08	0.99	0.98
Villemur, Tarn	Mean	0.88	0.94	0.92	0.88	0.89	0.93
	SD	0.05	0.02	0.05	0.15	0.07	0.03
	Min	0.82	0.90	0.85	0.70	0.79	0.88
	Max	0.97	0.96	0.98	1.07	0.99	0.97
Loubejac, Aveyron	Mean	0.79	0.89	0.87	0.89	0.84	0.93
	SD	0.10	0.07	0.13	0.20	0.11	0.04
	Min	0.69	0.81	0.73	0.66	0.71	0.88
	Max	0.98	0.99	1.08	1.08	0.99	0.97
Estirac, Adour	Mean	0.86	0.92	0.92	0.90	0.89	0.94
	SD	0.13	0.04	0.07	0.12	0.07	0.03
	Min	0.77	0.85	0.84	0.77	0.78	0.90
	Max	1.14	0.96	1.06	1.10	1.00	0.98
Aire, Adour	Mean	0.86	0.92	0.92	0.91	0.90	0.93
	SD	0.13	0.04	0.09	0.14	0.07	0.03
	Min	0.77	0.87	0.84	0.77	0.80	0.89
	Max	1.15	0.97	1.12	1.17	1.03	0.98
Audon, Adour	Mean	0.87	0.92	0.92	0.91	0.90	0.93
	SD	0.12	0.04	0.10	0.17	0.09	0.04
	Min	0.79	0.88	0.83	0.76	0.80	0.89
	Max	1.12	0.97	1.11	1.24	1.07	0.99
St Vincent, Adour	Mean	0.90	0.95	0.94	0.93	0.92	0.95
	SD	0.10	0.07	0.11	0.15	0.10	0.07
	Min	0.80	0.86	0.84	0.74	0.80	0.86
	Max	1.03	1.06	1.11	1.19	1.07	1.05
Escos, Gave d'Oloron	Mean	0.87	0.92	0.91	0.89	0.89	0.92
	SD	0.10	0.05	0.09	0.14	0.08	0.05
	Min	0.80	0.85	0.82	0.76	0.81	0.85
	Max	1.08	0.97	1.09	1.14	1.04	0.99
Berenx, Gave de Pau	Mean	0.81	0.90	0.89	0.90	0.87	0.88
	SD	0.09	0.04	0.11	0.16	0.08	0.06
	Min	0.72	0.84	0.77	0.73	0.76	0.79
	Max	0.99	0.94	1.10	1.19	1.02	0.97
Bergerac, Dordoge	Mean	0.83	0.93	0.89	0.88	0.87	0.92
	SD	0.07	0.05	0.13	0.20	0.12	0.06
	Min	0.74	0.87	0.76	0.68	0.76	0.85
	Max	0.96	1.02	1.13	1.19	1.10	1.01

[a]These values were first calculated for each of the months between July and October and then averaged over the low-flow period. Finally, the same values were calculated for the mean minimal monthly discharge ratios simulated at each of the hydrometric stations.

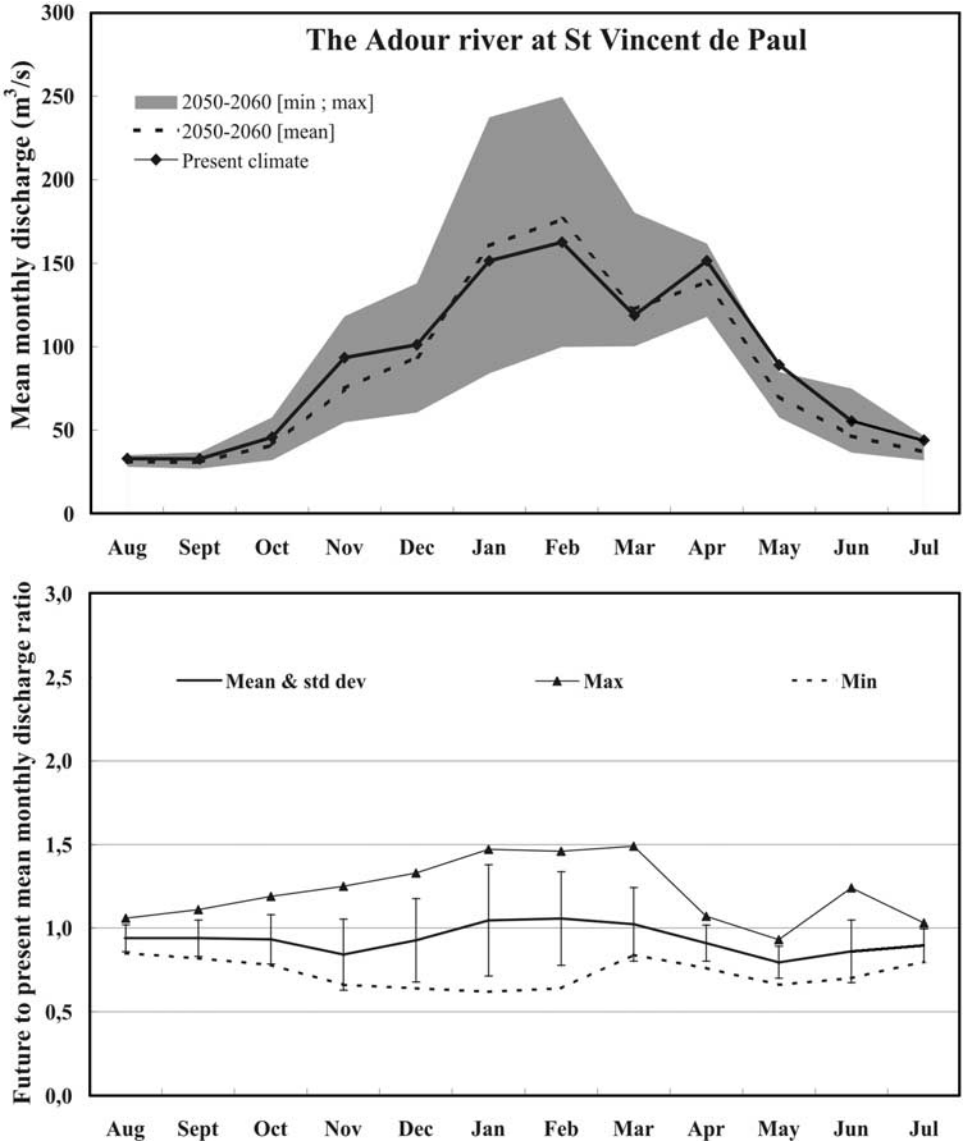

Figure 11. As in Figures 8 and 9, except for the Saint Vincent de Paul hydrometric station.

summarized as a temperature increase over the whole year and a precipitation increase in winter and a decrease in summer. The impact of the temperature increase and the precipitation decrease in summer is more significant and variable over a humid soil than over a dry soil in terms of river discharge, probably because of the larger availability of the soil's water content for the evapotranspiration processes. Evapotranspiration can be important over a humid soil, leading to a large reduction in the soil water content, while over a dry soil it is limited, leading to relatively constant soil water content. Consequently, for the wet year, as the soil water is lower in future climate conditions before the rainy season, it can store more water during the rain events, causing a higher reduction in river discharge in comparison to the present. Conversely, for the dry year, as the soil water content is almost unchanged, there are only slight differences in comparison to the present state.

[38] It can be concluded from the results presented in Table 4 that the climate change impacts could be higher, in a relative sense, for the low-flow period on river basins situated in wet climatic conditions, than for those under dry climatic conditions, if they are similar in terms of soil type and vegetation cover.

4.2. Impacts Simulated by the Continuous Scenario

[39] In order to analyze how fast the predicted climate change could modify hydrological processes in the future, it was helpful to use the data provided by the continuous scenario of the ARPEGE/IFS coupled ocean-atmospheric model [*Gibelin and Déqué*, 2003]. This scenario predicted the largest decrease in precipitation over the region of interest, because for this GCM, the trajectory of oceanic perturbations has shifted from west to southwest and are blocked by the Pyrenean range. Therefore the model simulated more precipitation in the southern part of the Pyrenees in Spain (windward side), and less in the French portion. The continuous scenario covers the 20-year 1985–

Table 4. Mean and Standard Deviation Values for the Low-Flow Period Simulated Discharge Ratios Between the Future and Present Wettest and Driest Years of the Decade Studied, Under All Scenarios for the Low-Flow Period

	Mean Ratio of Simulated Future to Present Discharge for the Low-Flow Period (Jul–Oct)		Standard Deviation	
Hydrometric Station	Wet Year	Dry Year	Wet Year	Dry Year
Foix	0.88	0.93	0.21	0.04
Auterive	0.87	0.93	0.25	0.05
Valentine	0.89	0.85	0.21	0.11
Roquefort	0.82	0.89	0.23	0.08
Portet	0.85	0.88	0.25	0.08
Lamagistère	0.84	0.89	0.23	0.07
Tonneins	0.81	0.88	0.22	0.06
Villemur	0.87	0.94	0.08	0.03
Loubejac	0.70	0.81	0.20	0.07
Estirac	0.85	0.89	0.24	0.11
Aire	0.86	0.88	0.28	0.12
Audon	0.88	0.89	0.27	0.09
St Vincent	0.87	0.94	0.21	0.09
Escos	0.84	0.90	0.26	0.07
Berenx	0.92	0.89	0.25	0.08
Bergerac	0.76	0.86	0.28	0.05
Mean values	0.84	0.89	0.23	0.08

2005 period, and it showed a general tendency for a discharge decrease over all seasons (Figure 12). This is mainly due to the precipitation decrease predicted by this scenario for almost all seasons and the entire simulation period, except in winter and spring for the 1995–2025 and 2045–2055 periods. The general decrease in the simulated solid precipitation and its variability, which are greater in spring through autumn than in winter, can be seen in Figure 12. The reduction in snow cover together with the increase in temperature induces an increase in the evaporation rate, which is stronger in winter than in spring. It is interesting to observe that the impacts of the 2025–2035 decade are of the same order as those simulated for the 2055–2065 decade. This was observed over all of the other hydrometric stations of the Adour-Garonne river basin and implies that the impacts estimated using the seven climate scenarios for the 2050–2060 decade could occur as early as 2020. However, the simulated evolution in the parameters presented for this continuous climate scenario are spatially variable over the Adour-Garonne river basin, as seen in sections 4.1.1 to 4.1.3, and there are substantial differences between the mountains and the plains. Moreover, it can be verified that a seasonal precipitation increase or decrease has strongly nonlinear impacts on the river discharge, depending on the season and decade considered. This underscores the complexity of the hydrometeorological processes driving river discharge production.

5. Conclusion

[40] This paper presents the results of a study conducted to investigate the possible impacts of climate change on the Adour-Garonne river basin. The future (2050–2060) and the present (1985–1995) simulated discharges were compared by calculating the mean monthly discharge ratios between the two decades. The analysis of the results of the climate scenario impacts on the water resources of the Adour-Garonne river basin leads to the following conclusions: An average 11% river discharge decrease over the river gauges of the whole basin was simulated during the low-flow period (July–October). The uncertainty associated with this climate change impact on the low-flow period is quite weak since all of the models simulate this reduction with relatively little variability (a standard deviation of 8% on average for all of the scenarios). The impact variability was found to be larger during the rest of the year, particularly during the wintertime, because of the uncertainty regarding the large variability between the scenarios. A decrease in the autumn discharges for the 2050–2060 decade was obtained, caused by the summer and autumn precipitation deficit. A substantial discharge increase during the winter (due to both the higher liquid precipitation caused by the increase in precipitation and temperature and to the lower snow cover storage) followed by a decrease during the spring (because of the earlier snowmelt due to higher temperatures) was simulated. The solid precipitation and the snow cover showed a significant decrease (approximately 50% for the snow depth and the snow cover duration simulated under the continuous climate scenario at the end of the century). As a consequence, the spring floods stemming from snowmelt were reduced and the low-flow period started 1 month earlier. The spring discharge deficit induced a stronger deficit in the July discharge in comparison with the rest of the low-flow period, for which the river was supplied by the groundwater base flow. The water storage of the groundwater reservoirs (the perched and alluvial groundwater sheet and the unconfined aquifer) was preserved owing to a significant winter recharge, greater than under the present climate. The relatively low impact of the climate scenarios on the low-flow period discharges of the 2050–2060 decade was a consequence of the substantial winter recharge. The simulated precipitation deficit during autumn was larger than the groundwater supply and therefore induced a larger discharge decrease.

[41] Comparing the simulated discharges for the wettest and driest years shows the stronger sensitivity of the wet year to the climate change scenarios (which is likely related

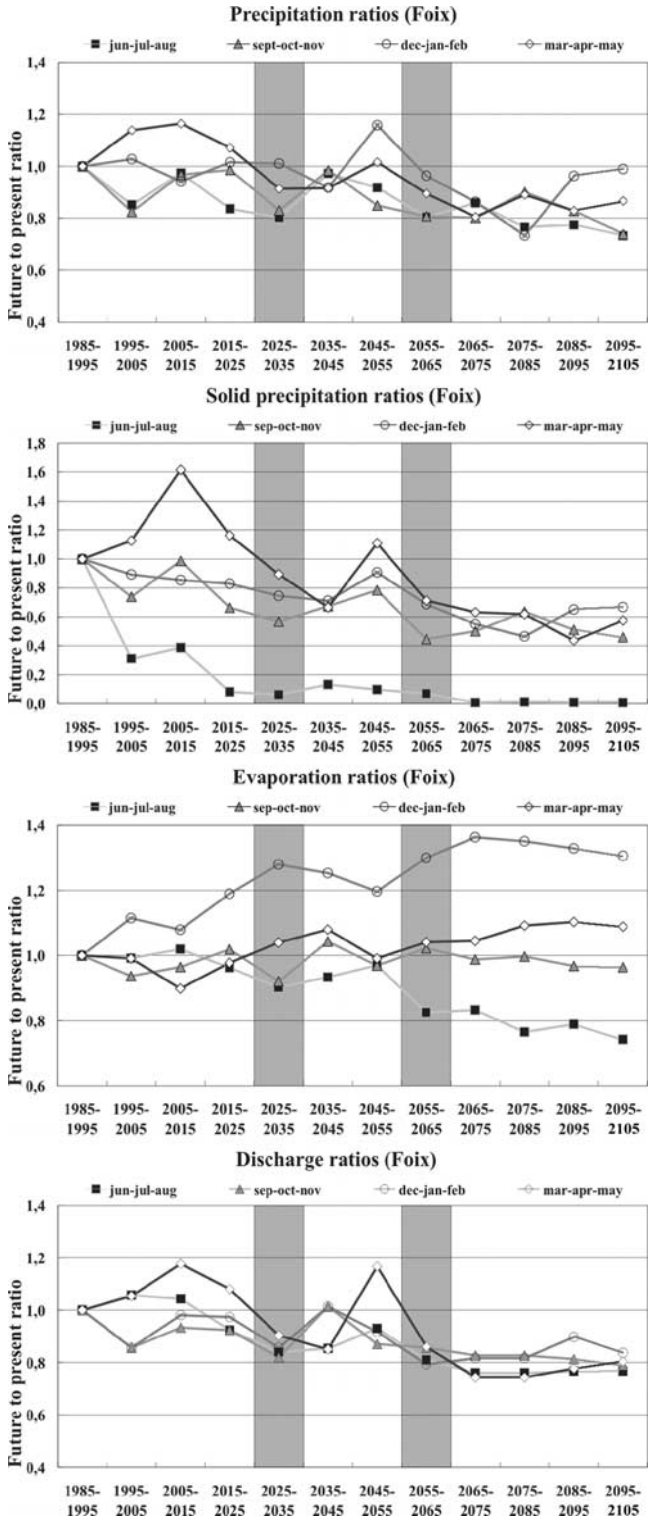

Figure 12. Evolution of the ratio of the mean seasonal total and solid precipitation, evaporation, and future discharge compared to present ratio values simulated under the continuous scenario averaged by decades for the Foix hydrometric station for the Ariège River basin.

to the soil water content control on the hydrological processes, particularly evapotranspiration). The continuous scenario provoked a general decrease in the river discharges over all the seasons from the present to 2100. This decrease results mainly from the precipitation reduction simulated by this scenario through the end of the century. The impact on the 2020–2030 decade was found to be on the same order as the impact for the 2050–2060 decade.

[42] Other studies obtained similar results in other basins [*Dettinger et al.*, 2004; *Gleick*, 1987; *Gleick and Chalecki*, 1999; *Lettenmaier and Gan*, 1990; *Miller et al.*, 2003; *VanRheenan et al.*, 2004; *Wolock and McCabe*, 1999], but few others have combined monthly temperature and precipitation anomalies calculated from several GCMs [*Etchevers et al.*, 2002; *Hamlet and Lettenmaier*, 1999; *Leung and Wigmosta*, 1999; *Maurer and Duffy*, 2005] with an integration of groundwater and SVAT models.

[43] Now state-of-the-art studies use either a wide range of different GCMs as well as emission scenarios [*Zierl and Bugmann*, 2005] or an overall simulation for a given GCM (ENSEMBLE, DISCENDO projects) together with downscaling methods to reduce the modeling structure's influence on the results and also to better assess the modeling system's uncertainties [*Booij*, 2005; *Maurer and Duffy*, 2005; *Boé et al.*, 2006]. Complementary work should also be done to improve the hydrological process analysis, such as a better simulation of the feedback between the soil water content and the groundwater aquifers and the assessment of the climate change impact on the soil water content, or an exploration of the impact of the extreme changes on hydrological processes. Finally, it is necessary to integrate modeling the vegetation's adaptation to the climate change, and changes in irrigation and farming management practices.

[44] **Acknowledgments.** The authors would like to thank the Adour-Garonne River Basin Water Management Agency (AGWA) for its financial support for this study. We also would like to thank the journal editors and three anonymous reviewers for their useful comments.

References

Allen, D. M., D. C. Mackie, and M. Wei (2004), Groundwater and climate change: A sensitivity analysis for the Grand Forks aquifer, southern British Columbia, Canada, *Hydrogeol. J.*, *13*(3), 270–290.

Arnell, N. W. (1999), The effect of climate change on hydrological regimes in Europe: A continental perspective, *Global Environ. Change*, *9*, 5–23.

Arnell, N. W., and N. S. Reynard (1996), The effects of climate change due to global warming on river flows in Great Britain, *J. Hydrol.*, *183*(397), 424.

Arnell, N. W., M. J. L. Livermore, S. Kovats, P. E. Levy, R. Nicholls, M. L. Parry, and S. R. Gaffin (2004), Climate and socio-economic scenarios for global-scale climate change impacts assessments: Characterising the SRES storylines, *Global Environ. Change*, *14*, 3–20, doi:10.1016/j.gloenvcha.2003.10.004.

Bobba, A. G., V. P. Singh, D. S. Jeffies, and L. Bengtsson (1997), Application of a watershed runoff model to north east Pond River, Newfoundland: To study water balance and hydrological characteristics owing to atmospheric change, *Hydrol. Processes*, *11*(12), 1573–1593.

Boé, J., L. Terray, F. Habets, and E. Martin (2006), A simple statistical-dynamical downscaling scheme based on weather types and conditional resampling, *J. Geophys. Res.*, *111*, D23106, doi:10.1029/2005JD006889.

Booij, M. J. (2005), Impact of climate change on river flooding assessed with different spatial model resolutions, *J. Hydrol.*, *303*(1–4), 176–198.

Boone, A., and P. Etchevers (2001), An inter-comparison of three snow schemes of varying complexity coupled to the same land-surface model: Local scale evaluation at an Alpine site, *J. Hydrometeorol.*, *2*, 374–394.

Boone, A., J. C. Calvet, and J. Noilhan (1999), Inclusion of a third soil layer in a land surface scheme using the force-restore method, *J. Appl. Meteorol.*, *38*, 1611–1630.

Boone, A., V. Masson, T. Meyers, and J. Noilhan (2000), The influence of the inclusion of soil freezing on simulations by a soil-vegetation-atmosphere transfer scheme, *J. Appl. Meteorol.*, *39*, 1544–1569.

Burn, D. H., and M. H. Hag Elnur (2002), Detection of hydrologic trends and variability, *J. Hydrol.*, *255*(1–4), 107–122.

Caballero, Y., and J. Noilhan (2003), Etude de l'impact hydrologique du changement climatique sur les ressources en eau du bassin Adour Garonne, 176 pp., Météo-France, Toulouse.

Chen, Z., S. E. Grasby, and K. G. Osadez (2004), Relation between climate variability and groundwater levels in the upper carbonate aquifer, southern Manitoba, Canada, *J. Hydrol.*, *290*(1–2), 43–62.

Courtier, P., and J.-F. Geleyn (1988), A global numerical weather prediction model with variable resolution: Application to the shallow-water equations, *Q.J.R. Meteorol. Soc.*, *114*, 1321–1346.

Dettinger, M. D., D. R. Cayan, M. K. Meyer, and A. E. Jeton (2004), Simulated responses to climate change variations and change in the Merced, Carson, and American river basins, Sierra Nevada, California 1900–2099, *Clim. Change*, *62*, 283–317.

Douville, H., E. Bazile, P. Caille, D. Giard, J. Noilhan, L. Peirone, and F. Taillefer (1999), Global soil wetness project, *J. Meteorol. Soc. Jpn.*, *77*(1B), 305–316.

Drogue, G., L. Pfister, T. Leviandier, A. El Idrissi, J.-F. Iffly, P. Matgen, J. Humbert, and L. Hoffmann (2004), Simulating the spatio-temporal variability of streamflow response to climate change scenarios in a mesoscale basin, *J. Hydrol.*, *293*, 255–269.

Durand, Y., E. Brun, L. Merindol, G. Guyomarc'h, B. Lesaffre, and E. Martin (1993), A meteorological estimation of relevant parameters for snow models, *Ann. Geophys.*, *18*, 65–71.

Etchevers, P., C. Golaz, and F. Habets (2001), Simulation of the water budget and the river flows of the Rhône basin from 1981 to 1994, *J. Hydrol.*, *244*, 60–85.

Etchevers, P., C. Golaz, F. Habets, and J. Noilhan (2002), Impact of a climate change on the Rhone River catchment hydrology, *J. Geophys. Res.*, *107*(D16), 4293, doi:10.1029/2001JD000490.

Gellens, D., and B. Schädler (1997), Comparaison des réponses du bilan hydrique de bassins situés en Belgique et en Suisse à un changement de climat, *Rev. Sci. Eau*, *10*(3), 395–414.

Gibelin, A. L., and M. Déqué (2003), Anthropogenic climate change over the Mediterranean region simulated by a global variable resolution model, *Clim. Dyn.*, *20*, 327–339.

Gleick, P. H. (1987), The development and testing of a water balance model for climate impact assessment: Modeling the Sacramento basin, *Water Resour. Res.*, *23*(6), 1049–1061.

Gleick, P. H., and E. L. Chalecki (1999), The impacts of climatic changes for water resources of the Colorado and Sacramento-San Joaquin river basins, *J. Am. Water Resour. Assoc.*, *35*(6), 1429–1441.

Gregory, J. M., J. F. B. Mitchell, and A. J. Brady (1997), Summer drought in northern midlatitudes in a time-dependent CO2 climate experiment, *J. Clim.*, *10*(4), 662–686.

Habets, F., P. Etchevers, C. Golaz, E. Leblois, E. Ledoux, E. Martin, J. Noilhan, and C. Ottle (1999a), Simulation of the water budget and the river flows of the Rhone basin, *J. Geophys. Res.*, *104*, 31,145–31,172.

Habets, F., J. Noilhan, C. Golaz, J. P. Goutorbe, P. Lacarrere, E. Leblois, E. Ledoux, E. Martin, C. Ottle, and D. Vidal-Madjar (1999b), The Isba surface scheme in a macroscale hydrological model applied to the Hapex-Mobilhy area. part I: Model and database, *J. Hydrol.*, *217*, 75–96.

Habets, F., J. Noilhan, C. Golaz, J. P. Goutorbe, P. Lacarrere, E. Leblois, E. Ledoux, E. Martin, C. Ottle, and D. Vidal-Madjar (1999c), The Isba surface scheme in a macroscale hydrological model applied to the Hapex-Mobilhy area. part II: Simulation of streamflows and annual water budget, *J. Hydrol.*, *217*, 97–118.

Hamlet, A. F., and D. P. Lettenmaier (1999), Effects of climate change on hydrology and water resources in the Columbia River basin, *J. Am. Water Resour. Assoc.*, *35*(6), 1597–1624.

Houghton, J. T., Y. Ding, D. J. Griggs, M. Noguer, P. J. Van der Linden, X. Da, K. Maskell, and C. A. Johnson (Eds.) (2001), *Climate Change 2001: The Scientific Basis*, 944 pp., Cambridge Univ. Press, Cambridge, U. K.

Ledoux, E., G. Girard, G. De Marsily, and J. Deschenes (1989), Spatially distributed modeling: Conceptual approach, coupling surface water and ground-water, in *Unsaturated Flow Hydrologic Modeling: Theory and Practice*, edited by H. J. Morel-Seytoux, pp. 435–454, Springer, New York.

Lehenaff, A. (2002), Impact du changement climatique sur la ressource en eau du bassin Adour Garonne, 58 pp., Ecole Nationale de Météorologie, Météo-France, Toulouse.

LeMoigne, P. (2002), Description de l'analyse des champs de surface sur la France par le système SAFRAN, Météo-France, Toulouse.

Lettenmaier, D. P., and T. Y. Gan (1990), Hydrologic sensitivities of the Sacramento-San Joaquin river basin, California, to global warming, *Water Resour.Res.*, *26*(1), 69–86.

Leung, L. R., and M. S. Wigmosta (1999), Potential climate change impacts on mountain watersheds in the Pacific Northwest, *J. Am. Water Resour. Assoc.*, *35*(6), 1463–1471.

Mahfouf, J.-F., and J. Noilhan (1996), Inclusion of gravitational drainage in a land surface scheme based on the force-restore method, *J. Appl. Meteorol.*, *35*, 987–992.

Martin, E. (2000), Modification du cycle hydrologique: Modification de la couverture neigeuse, in *Impact potentiel du changement climatique en France au XXIe siècle*, pp. 54–57, *Mission interminist. sur l'effet de serre*, Paris. (Available online at http://www.effet-de-serre.gouv.fr/images/documents/Impactpotentielfrancepartie2.pdf)

Masson, V., J. L. Champeaux, F. Chauvin, C. Meriguet, and R. Lacaze (2003), A global database of land surface parameters at 1 km resolution in meteorological and climate models, *J. Clim.*, *16*, 1261–1282.

Maurer, E. P., and P. B. Duffy (2005), Uncertainty in projections of streamflow changes due to climate change in California, *Geophys. Res. Lett.*, *32*, L03704, doi:10.1029/2004GL021462.

McCabe, G. J., and L. E. Hay (1995), Hydrologic effects of hypothetical climate changes on water resources in the East River basin, Colorado, *Hydrol. Sci. J.*, *40*, 303–318.

Miller, N. L., K. E. Bashford, and E. Strem (2003), Potential impacts of climate change on California hydrology, *J. Am. Water Resour. Assoc.*, *39*, 771–784.

Milly, P. C. D., R. T. Wetherald, K. A. Dune, and T. L. Delworth (2002), Increasing of great floods in a changing climate, *Nature*, *415*, 514–517.

Moisselin, J.-M., M. Schneider, C. Canellas, and O. Mestre (2002), Les changements climatiques en France au 20eme siècle en France, *Meteorologie*, *38*, 45–56.

Morin, G., and M. Slivitzky (2002), Impacts des changements climatiques sur le régime hydrologique: le cas de la rivière Moisie, *Rev. Sci. Eau*, *5*, 179–195.

Nash, J. E., and J. V. Sutcliffe (1970), River flow forecasting through conceptual models, *J. Hydrol.*, *10*(3), 282–290.

Nash, L. L., and P. H. Gleick (1991), Sensitivity of streamflow in the Colorado basin to climatic changes, *J. Hydrol.*, *125*(3–4), 221–241.

Noilhan, J., and J.-F. Mahfouf (1996), The ISBA land surface parameterization scheme, *Global Planet. Change*, *13*, 145–159.

Noilhan, J., and S. Planton (1989), A simple parameterization of land surface processes for meteorological models, *Mon. Weather Rev.*, *117*, 536–549.

Noilhan, J., A. Boone, and P. Etchevers, (2001), Application of climate change scenarios to the Rhone basin, in *Applying Climate Scenarios for Regional Studies: With Particular Reference to the Mediterranean, ECLAT-2 Toulouse Workshop Report 4, France, 25–27 October 2000*, pp. 58–74, Clim. Res. Unit UEA, Norwich, U. K.

Palmer, T. N., and J. Räisänen (2002), Quantifying the risk of extreme seasonal precipitation events in a changing climate, *Nature*, *415*, 512–514.

Polcher, J., J. F. Crossley, C. Bunton, H. Douville, N. Gedney, K. Laval, S. Planton, P. R. Rowntree, and P. Valdes (1998), Importance of land-surface processes for the uncertainties of climate change: A European project, *GEWEX News*, *8*(2), 11–13.

Romero, R., C. Ramis, J. A. Guijarro, and S. Alonso (1998), A 30-year (1964–1993) daily rainfall data base for the Spanish Mediterranean regions: First exploratory study, *Int. J. Climatol.*, *18*, 541–560.

Rosenberg, N. J., D. J. Epstein, D. Wang, L. Vail, R. Srinivasan, and J. G. Arnold (1999), Possible impacts of global warming on the hydrology of the Ogallala aquifer region, *Clim. Change*, *42*(4), 677–692.

Rousset, F., F. Habets, E. Gomez, P. LeMoigne, S. Voirin-Morel, J. Noilhan, and E. Ledoux (2004), Hydrometeorological modeling of the Seine basin using the SAFRAN-ISBA-MODCOU system, *J. Geophys. Res.*, *109*, D14105, doi:10.1029/2003JD004403.

Roy, L., R. Leconte, F. P. Brisstte, and C. Marche (2001), The impact of climate change on seasonal floods of a southern Quebec River basin, *Hydrol. Processes*, *15*(16), 3167–3179.

Stewart, I. T., D. R. Cayan, and M. D. Dettinger (2005), Changes toward earlier streamflow timing across western North America, *J. Clim.*, *18*, 1136–1155.

VanRheenan, N. T., A. W. Wood, R. N. Palmer, and D. P. Lettenmaier (2004), Potential implications of PCM climate change scenarios for Sacramento-San Joaquin river basin hydrology and water resources, *Clim. Change*, *62*, 257–281.

Voirin-Morel, S. (2003), Modélisation distribuée des flux d'eau et d'énergie et des débits à l'échelle régionale du bassin Adour Garonne, Ph.D. thesis, 292 pp., Univ. Paul Sabatier-Toulouse III, Toulouse, France. (Available at http://www.cig.ensmp.fr/∼hydro/THE/the.htm)

Wolock, D. M., and G. J. McCabe (1999), Estimates of runoff using water-balance and atmospheric general circulation models, *J. Am. Water Resour. Assoc.*, *35*(6), 1341–1350.

Xu, C.-Y. (1999), From GCMs to river flow: A review of downscaling methods and hydrologic modelling approaches, *Prog. Phys. Geogr.*, *23*(2), 229–249.

Zhang, X., K. D. Harvey, W. D. Hogg, and T. R. Yuzik (2001), Trends in Canadian streamflow, *Water Resour. Res.*, *37*(4), 987–999.

Zierl, B., and H. Bugmann (2005), Global change impacts on hydrological processes in Alpine catchments, *Water Resour. Res.*, *41*, W02028, doi:10.1029/2004WR003447.

A. Boone, A. Lehenaff, P. LeMoigne, and J. Noilhan, CNRM Météo-France, 42 avenue Coriolis, 31057 Toulouse Cedex 1, France.

Y. Caballero, French Geological Survey (BRGM), Immeuble Agostini, Z.I. de Furiani, 20600 Bastia, France. (y.caballero@brgm.fr)

F. Habets, UMR Sisyphe ENSMP, 35 rue St. Honoré, 77305 Fontainebleau, France.

S. Voirin-Morel, Direction of Climatology, Météo-France, 42 avenue Coriolis, 31057 Toulouse Cedex 1, France.